Supplemental Data

Cu(II) mediates kinetically distinct, non-amyloidogenic aggregation of amyloid-β peptides

Jeppe T. Pedersen[1], Jesper Østergaard[1], Noemi Rozlosnik[2], Bente Gammelgaard[1], Niels H. H. Heegaard[3]

Affiliations:

[1]Department of Pharmaceutics and Analytical Chemistry, Faculty of Pharmaceutical Sciences, University of Copenhagen, Universitetsparken 2, DK-2100 Copenhagen, Denmark. [2]Department of Micro- and Nanotechnology, Technical University of Denmark, Ørsted plads, DK-2800 Kongens Lyngby, Denmark. [3]Department of Clinical Biochemistry and Immunology, Statens Serum Institut, Artillerivej 5, DK-2300 Copenhagen, Denmark.

Correspondence should be addressed to J. Ø. (joe@farma.ku.dk) or N. H. H. H. (nhe@ssi.dk)

SUPPLEMENTAL METHODS

Models and data fitting. Concentration-time (CE data) or fluorescence-time (ThT data) profiles were fitted to four different models.

2-step autocatalytic growth model. Finke and Watzky proposed a minimal mathematical model to describe protein aggregation kinetics (1). Here any monomer (P) is irreversibly converted to an aggregated form (F). This aggregate form can then react with another monomer P as depicted in Scheme 1.

$$\mathrm{P} \xrightarrow{k_1} \mathrm{F}$$

$$\mathrm{P} + \mathrm{F} \xrightarrow{k_2} 2\,\mathrm{F}$$

Scheme 1 Reaction mechanism for 2-step autocatalytic growth model

The concentration of monomeric P at time t, $[P]_t$, is mathematically described by**:**

$$[\mathrm{P}]_t = \frac{k_1 + k_2[\mathrm{P}]_0}{k_2 + \frac{k_1}{[\mathrm{P}]_0}\exp\left[(k_1 + k_2[\mathrm{P}]_0)t\right]} \qquad (\mathrm{S1}A)$$

where $[P]_0$, k_1 and k_2 are the initial monomer concentration, rate constant of nucleation, and rate constant of growth, respectively. Equation S1*A* was applied to the CE data.
The corresponding expression for the formation of aggregates is:

$$[\mathrm{F}]_t = [\mathrm{P}]_0 - \frac{k_1 + k_2[\mathrm{P}]_0}{k_2 + \frac{k_1}{[\mathrm{P}]_0}\exp\left[(k_1 + k_2[\mathrm{P}]_0)t\right]} \qquad (\mathrm{S1}B)$$

Eq. S1*B* was applied to the ThT data.

Kinetic data not consistent with the 2-step autocatalytic growth model were fitted to a first order polynomial model (apparent zero order kinetics), single exponential model (apparent first order kinetics), and a sum of two exponentials. These should be

considered entirely as mathematical models describing the kinetic data and were used to attain measures of the aggregation rates, *i.e.*, Eq. S2-5.

$$[\mathrm{P}]_t = k_1 t + [\mathrm{P}]_0 \tag{S2}$$

$$[\mathrm{P}]_t = [\mathrm{P}]_0 \exp(-k_1 t) \tag{S3}$$

$$[\mathrm{P}]_t = [P]_0 \left\{ f_{fast} \exp(-k_1 t) + (1 - f_{fast}) \exp(-k_2 t) \right\} \tag{S4}$$

$$[P]_t = [P]_\infty + \left([P]_0 - [P]_\infty \right) \exp\left[-k_1 (t - t_0) \right] \tag{S5}$$

The aggregation described by Eq. S4 is characterized by a fast and a slow phase, where the constant f_{fast} is the fraction of the curve accounted for by the fast phase. The aggregation described by Eq. S5 is characterized by a time-interval t_0 prior to a mono-exponential decrease in the soluble peptide concentration, and the presence of a plateau concentration $[P]_\infty$ at infinite times, i.e. a fraction of soluble peptide that apparently remains in solution.

Data from the experiments characterizing Cu(II) induced aggregation were fitted to the Eqs. S1-5. The goodness of the fit was evaluated visually by inspection of the curves and residual plots, and through the size of the s.e.m. of the fitted parameters. Model discrimination was carried out by visual comparison of the fits and by evaluation of the corrected Akaike's Information Criterion (AIC_C) (2). The AIC_C was calculated from the residual sum of squares (*RSS*), the number of data points *N*, and the number of fitted parameters plus one (*K*) using:

$$\mathrm{AIC}_C = N \ln\left(\frac{RSS}{N} \right) + 2K + \frac{2K(K+1)}{N - K - 1} \tag{S6}$$

The probability that the model with the best fit was correct compared to another model *i* (with a poorer fit), is based on their difference in AIC_C score, $\Delta\mathrm{AIC}_C = \mathrm{AIC}_{C,i} - \mathrm{AIC}_{C,\text{best fit}}$, and is calculated by:

$$\text{probability} = \frac{\exp(-0.5\Delta\text{AIC}_C)}{1+\exp(-0.5\Delta\text{AIC}_C)} \qquad \text{(S7)}$$

Although the 2-step autocatalytic growth model and the associated rate constants provide some mechanistic insight into the aggregation event it is primarily used in this study as a mathematical model in order to discriminate between spontaneous and Cu(II) induced aggregation. When Eq. S1 did not fit the data it was assumed that the underlying aggregation mechanism was incompatible with the 2-step autocatalytic growth model.

Numerical simulations. The differential equation describing the kinetic flux for each species X_i in a general one-step kinetic reaction involving N chemical species:

$$a_1X_1 + \ldots + a_NX_N \underset{k_{-1}}{\overset{k_{+1}}{\rightleftharpoons}} b_1X_1 + \ldots b_NX_N$$

is given by (3):

$$\frac{d[X_i]}{dt} = \left[k_{+1}\prod_{j=1}^{N}\left([X_j]^{a_j}\right) - k_{-1}\prod_{j=1}^{N}\left([X_j]^{b_j}\right)\right] \times (b_i - a_i) \qquad \text{(S8)}$$

where a_j and b_j are the stoichiometric constants for the jth specie on the left- and right-hand side of the reaction, respectively. For a multi-step reaction consisting of M steps the differential equation for each species X_i is a sum:

$$\frac{d[X_i]}{dt} = \sum_{h=1}^{M}\left[k_{+h}\prod_{j=1}^{N}\left([X_j]^{a_{j,h}}\right) - k_{-h}\prod_{j=1}^{N}\left([X_j]^{b_{j,h}}\right)\right] \times (b_{i,h} - a_{i,h}) \qquad \text{(S9)}$$

Based on the model proposed in manuscript Fig. 4, we simulated the kinetic curves for the decrease in soluble Aβ and Cu(II) (manuscript Fig. 5 and Table S2).

SUPPLEMENTAL FIGURES

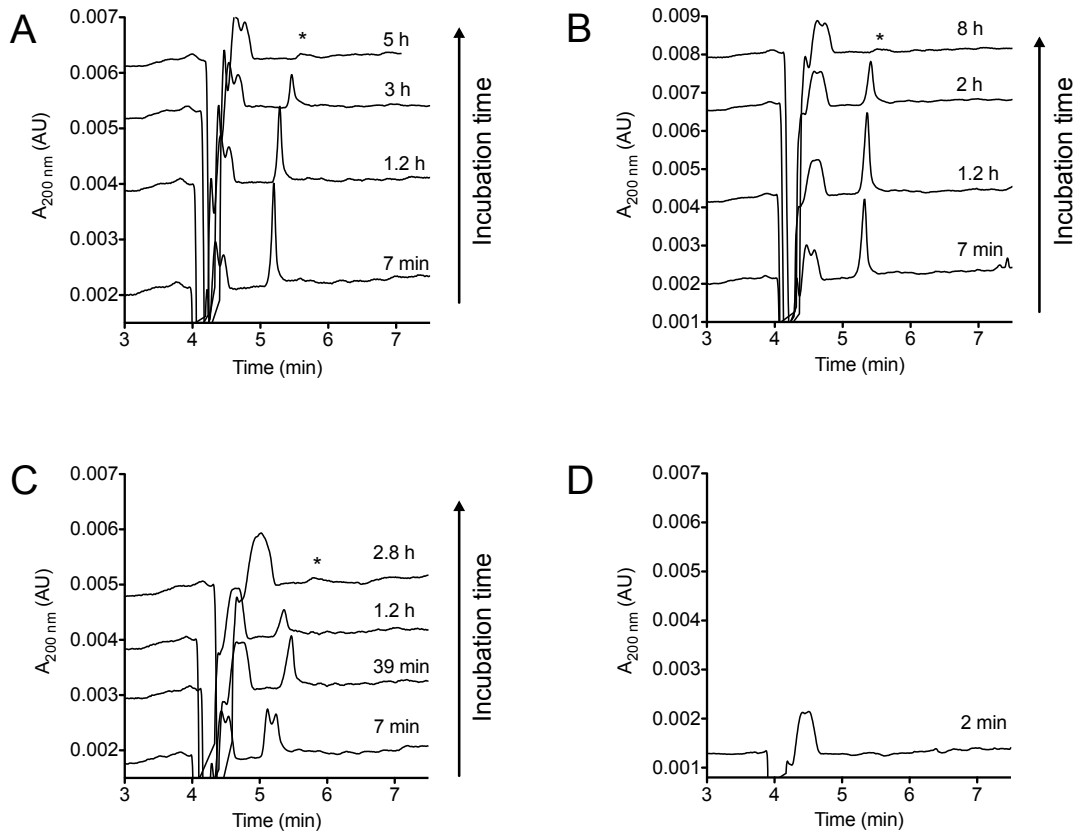

FIGURE S1. **Electropherograms at various times after incubation showing the disappearance of soluble Aβ$_{1-42}$ in water at pH 10.5 and 37°C.** *A*, electropherograms of apo-Aβ$_{1-42}$ (40 μM). *B*, electropherograms of Aβ$_{1-42}$ (40 μM) after incubation with 10 μM Cu(II). *C*, electropherograms of Aβ$_{1-42}$ (40 μM) after incubation with 40 μM Cu(II). *D*, electropherograms of Aβ$_{1-42}$ (40 μM) after incubation with 200 μM Cu(II).

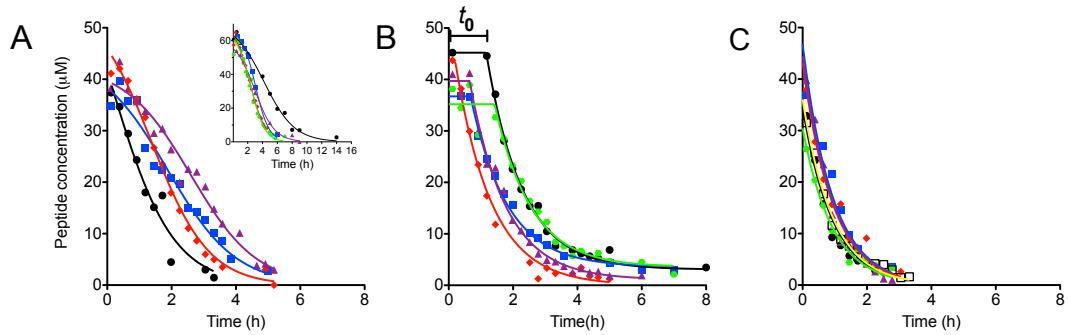

FIGURE S2. **Disappearance kinetics of soluble Aβ$_{1-42}$ in water at pH 10.5 and 37°C.** *A*, disappearance kinetics of soluble Aβ$_{1-42}$ (40 μM). *Inset*, disappearance kinetics of soluble apo-Aβ$_{1-40}$ (60 μM). *B*, disappearance kinetics of soluble Aβ$_{1-42}$ (40 μM) in the presence of 10 μM Cu(II). *C*, disappearance kinetics of soluble Aβ$_{1-42}$ (40 μM) after addition of 40 μM Cu(II). Data are fitted to supplemental Eq. S1 (*A*), Eq. S5 (*B*) and Eq. S3 (*C*). The time t_0 before the aggregation begins is highlighted in *B*. See also Table S1. The experimental conditions were the same as in Fig. S1.

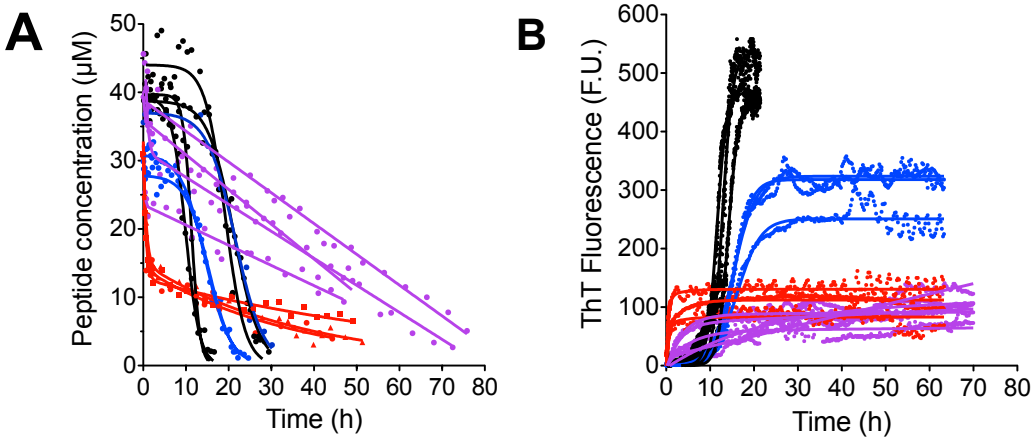

FIGURE S3. **Kinetic profiles for all CE and ThT repetitions with $A\beta_{1\text{-}40}$.** *A*, disappearance kinetics of soluble $A\beta_{1\text{-}40}$ (40 μM) in the absence (•) and in the presence of 10 μM (■), 40 μM (▲), and 200 μM (◆) Cu(II). Data are fitted to Eq. S1 (0 and 10 μM), Eq. S2 (40 μM) and Eq. S4 (200 μM). *B*, fibril formation kinetics of $A\beta_{1\text{-}40}$ (40 μM) in the absence (•) and in the presence of 10 μM (■), 40 μM (▲), and 200 μM (◆) Cu(II). The experimental conditions were the same as in manuscript Fig. 1.

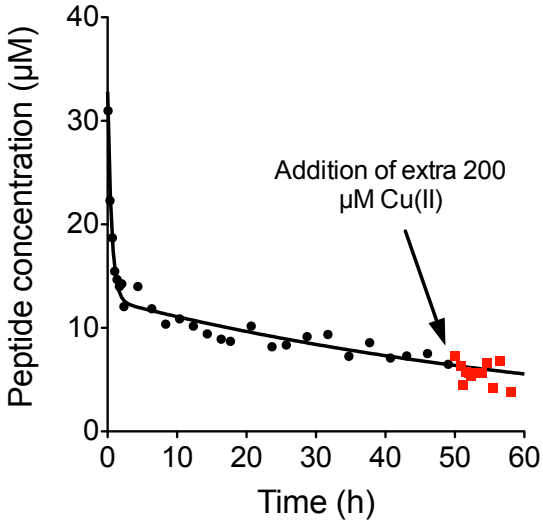

FIGURE S4. **Influence of additional 200 μM Cu(II) on the disappearance kinetics of $A\beta_{1\text{-}40}$ (40 μM) incubated with 200 μM Cu(II)**. (•) are CE data before the addition of 200 μM extra Cu(II). (■) are CE data after the addition of 200 μM extra Cu(II). Only data before the addition of extra Cu(II) was fitted to Eq. S4 and then extrapolated to 60 h. The additional Cu(II) does not cause an additional fast decrease in soluble $A\beta_{1\text{-}40}$, indicating that $A\beta_{1\text{-}40}$ present in solution is already fully loaded with Cu(II).

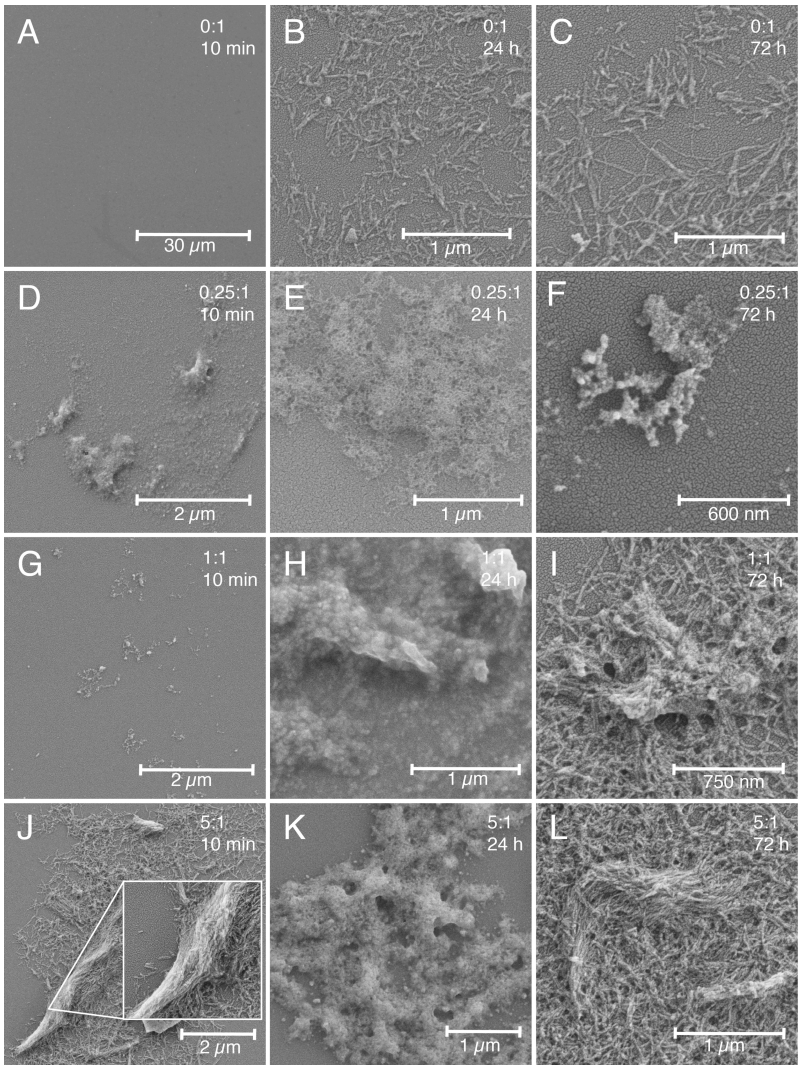

FIGURE S5. **SEM pictures of 40 μM A$\beta_{1\text{-}40}$ at different metal:peptide ratios and incubation times.** Fibrils were detected after 24 h in the absence of Cu(II) (*B*). Aggregates were seen immediately after addition of Cu(II) (*D*, *G*, and *J*). The Cu(II) induced aggregates appeared more heterogeneous than the fibrils. The experimental conditions were the same as in manuscript Fig. 1.

SUPPLEMENTAL TABLES

Table S1 Fitted parameters for the aggregation of $A\beta_{1-42}$ (40 μM) with and without added Cu(II) (10-200 μM). The experiments were performed at 37°C in water at pH 10.5. The aggregation of $A\beta_{1-42}$ was detected with CE. Rate constants are best-fitted values ± s.e.m, while t_0 is average ± s.d. The range of the individual best fit is listed in brackets for k_1 in the 2-phase autocatalytic (AC) model. n is the number of individual experiments. For the 2-phase AC model k_1 is the rate constant of nucleation, and k_2 is the rate constant of fibril growth. For both mono-exponential models k_1 is the 1st order rate constant. t_0 is the time before the exponential decay starts at 0.25 Cu(II):$A\beta_{1-42}$ ratio.

Cu(II):$A\beta_{1-42}$ ratio	Model	k_1 s^{-1}	k_2 $\mu M^{-1}\ s^{-1}$	t_0 min
0	2-phase AC[a] (n = 4)[d]	$[2.1 \times 10^{-5} – 2.6 \times 10^{-4}]$	$(6.8 \pm 0.6) \times 10^{-6}$	–
0.25	plateau + mono-exp[b] (n = 5)[d]	$(2.5 \pm 0.1) \times 10^{-4}$	–	50 ± 29
1	mono-exp[c] (n = 6)[d]	$(3.0 \pm 0.1) \times 10^{-4}$	–	–
5	No fit – peptide completely aggregated prior to the first measurement (~2 min)	–	–	–

[a] Supplemental Eq. S1
[b] Supplemental Eq. S5
[c] Supplemental Eq. S3
[d] Global fit

TABLE S2 Models, differential equations and rate constants used to simulate the kinetic profiles in manuscript **Fig. 5**.

Cu:Aβ[a]	Model	Differential equations	Rate constants in simulation
0	$\mathrm{P} \xrightarrow{k_1} \mathrm{F}$ $\mathrm{P} + \mathrm{F} \xrightarrow{k_2} 2\ \mathrm{F}$	$\frac{\mathrm{d}[\mathrm{P}]}{\mathrm{d}t} = -k_1[\mathrm{P}] - k_2[\mathrm{P}][\mathrm{F}]$	$k_1 = 10^{-8}$ s^{-1} (based on data from this study) $k_2 = 6$ M^{-1} s^{-1} (based on data from this study)
< 1[b]	$\mathrm{P} \xrightarrow{k_1} \mathrm{F}$ $\mathrm{P} + \mathrm{F} \xrightarrow{k_2} 2\ \mathrm{F}$ $\mathrm{P} + \mathrm{M} \underset{k_{-3}}{\overset{k_3}{\rightleftharpoons}} \mathrm{PM}$ $\mathrm{PM} + \mathrm{PM} \xrightarrow{k_4} \mathrm{C}$ $\mathrm{C} \xrightarrow{k_5} \mathrm{A}$	$\frac{\mathrm{d}[\mathrm{P}]}{\mathrm{d}t} = k_{-3}[\mathrm{PM}] - k_1[\mathrm{P}] - k_2[\mathrm{P}][\mathrm{F}] - k_3[\mathrm{P}][\mathrm{M}]$ $\frac{\mathrm{d}[\mathrm{M}]}{\mathrm{d}t} = k_{-3}[\mathrm{PM}] - k_3[\mathrm{P}][\mathrm{M}]$ $\frac{\mathrm{d}[\mathrm{PM}]}{\mathrm{d}t} = k_3[\mathrm{P}][\mathrm{M}] - k_{-3}[\mathrm{PM}] - k_4[\mathrm{PM}]^2$ $\frac{\mathrm{d}[\mathrm{C}]}{\mathrm{d}t} = k_4[\mathrm{PM}]^2 - k_5[\mathrm{C}]$	$k_1 = 10^{-8}$ s^{-1} (based on data from this study) $k_2 = 6$ M^{-1} s^{-1} (based on data from this study) $k_3 = 10^7$ M^{-1} s^{-1} $k_{-3} = 0.1$ s^{-1} $k_4 = 2 \times 10^3$ M^{-1} s^{-1} (lower limit) $k_5 = 5 \times 10^{-3}$ s^{-1} (lower limit)
= 1	$\mathrm{P} + \mathrm{M} \underset{k_{-1}}{\overset{k_1}{\rightleftharpoons}} \mathrm{PM}$ $\mathrm{PM} + \mathrm{PM} \xrightarrow{k_2} \mathrm{C1}$ $\mathrm{C1} \underset{k_{-3}}{\overset{k_3}{\rightleftharpoons}} \mathrm{C2}$ $\mathrm{C1} \xrightarrow{k_4} \mathrm{A}$	$\frac{\mathrm{d}[\mathrm{P}]}{\mathrm{d}t} = \frac{\mathrm{d}[\mathrm{M}]}{\mathrm{d}t} = k_{-1}[\mathrm{PM}] - k_1[\mathrm{P}][\mathrm{M}]$ $\frac{\mathrm{d}[\mathrm{PM}]}{\mathrm{d}t} = k_1[\mathrm{P}][\mathrm{M}] - k_{-1}[\mathrm{PM}] - k_2[\mathrm{PM}]^2$ $\frac{\mathrm{d}[\mathrm{PM}]}{\mathrm{d}t} = k_1[\mathrm{P}][\mathrm{M}] - k_{-1}[\mathrm{PM}] - k_2[\mathrm{PM}]^2$ $\frac{\mathrm{d}[\mathrm{C2}]}{\mathrm{d}t} = k_3[\mathrm{C1}] - k_{-3}[\mathrm{C2}]$	$k_1 = 10^7$ M^{-1} s^{-1} $k_{-1} = 0.1$ s^{-1} $k_2 = 10^3$ M^{-1} s^{-1} (lower limit) $k_3 = 20$ s^{-1} ($k_3/k_3 \geq 10^5$, and $k_3 \geq 10$ s^{-1}) $k_{-3} = 2 \times 10^{-4}$ s^{-1} $k_4 = 0.4$ s^{-1} [~ 0.2-0.6 s^{-1}]

Table S2 (cont.)

Cu:Aβ	Model	Differential equations	Rate constants in simulation
>1[c]	$\mathrm{P} + \mathrm{M} \underset{k_{-1}}{\overset{k_1}{\rightleftharpoons}} \mathrm{PM}$	$\frac{\mathrm{d[P]}}{\mathrm{d}t} = k_{-1}[\mathrm{PM}] - k_1[\mathrm{P}][\mathrm{M}]$	$k_1 = 10^7\ \mathrm{M^{-1}\ s^{-1}}$
	$\mathrm{PM} + \mathrm{M} \underset{k_{-2}}{\overset{k_2}{\rightleftharpoons}} \mathrm{PMM}$	$\frac{\mathrm{d[M]}}{\mathrm{d}t} = k_{-1}[\mathrm{PM}] + k_{-2}[\mathrm{PMM}] - (k_1[\mathrm{P}] + k_2[\mathrm{PM}])[\mathrm{M}]$	$k_{-1} = 0.1\ \mathrm{s^{-1}}$
			$k_2 = 2.9 \times 10^4\ \mathrm{M^{-1}\ s^{-1}}$ ($k_2 \geq 5 \times 10^3\ \mathrm{M^{-1}\ s^{-1}}$)
	$\mathrm{PM} + \mathrm{PM} \xrightarrow{k_3} \mathrm{C1}$	$\frac{\mathrm{d[PM]}}{\mathrm{d}t} = k_1[\mathrm{P}][\mathrm{M}] + k_{-2}[\mathrm{PMM}]$	$k_{-2} = 1\ \mathrm{s^{-1}}$ ($k_2/k_{-2} \sim 10^4$-$10^5\ \mathrm{M^{-1}}$)
	$\mathrm{PMM} + \mathrm{PM} \xrightarrow{k_4} \mathrm{C1}$	$- (k_{-1} + k_2[\mathrm{M}] + k_3[\mathrm{PM}] + k_4[\mathrm{PMM}])[\mathrm{PM}]$	$k_3 \sim k_4 \sim [5 \times 10^3$-$10^5\ \mathrm{M^{-1}\ s^{-1}}]$
	$\mathrm{C1} \underset{k_{-5}}{\overset{k_5}{\rightleftharpoons}} \mathrm{C2}$	$\frac{\mathrm{d[PMM]}}{\mathrm{d}t} = k_2[\mathrm{PM}][\mathrm{M}] - (k_{-2} + k_4[\mathrm{PM}])[\mathrm{PMM}]$	$k_5 = 3.3 \times 10^{-5}\ \mathrm{s^{-1}}$ ($k_5/k_{-5} \sim 10^{-2}$, $k_5 \geq 10^{-5}\ \mathrm{s^{-1}}$)
	$\mathrm{C2} \xrightarrow{k_6} \mathrm{A}$	$\frac{\mathrm{d[C1]}}{\mathrm{d}t} = k_3[\mathrm{PM}]^2 + k_4[\mathrm{PM}][\mathrm{PMM}] + k_{-5}[\mathrm{C2}] - k_5[\mathrm{C1}]$	$k_{-5} = 4.7 \times 10^{-3}\ \mathrm{s^{-1}}$
		$\frac{\mathrm{d[C2]}}{\mathrm{d}t} = k_5[\mathrm{C1}] - (k_{-5} + k_6)[\mathrm{C2}]$	$k_6 = 2.0 \times 10^{-3}\ \mathrm{s^{-1}}$ (~1-3 × $10^{-3}\ \mathrm{s^{-1}}$)

[a] [P] = 40 μM in all simulations
[b] [M] = 10 μM
[c] [M] = 200 μM
P, monomeric peptide, F; catalytic fibril, M, metal; PM; metal-peptide complex; C, C1, and C2, metal-peptide oligomers; A, metal-peptide aggregates; PMM, metal-peptide-metal complex.

SUPPLEMENTAL REFERENCES

1. Morris, A. M., Watzky, M. A., Agar, J. N., and Finke, R. G. (2008) *Biochemistry* **47**, 2413-2427
2. Hurvich, C. M., and Tsai, C. L. (1989) *Biometrika* **76**, 297-307
3. Barshop, B. A., Wrenn, R. F., and Frieden, C. (1983) *Anal. Biochem.* **130**, 134-145
4. Faller, P. (2009) *Chembiochem* **10**, 2837-2845
5. Frieden, C. (1985) *Annu. Rev. Biophys. Biophys. Chem.* **14**, 189-210